

Comparison of Physicochemical and Bioactive Properties of Polysaccharides from Massa Medicata Fermentata and Its Processed Products

Shuang Liu, Long Chen, Wenjuan Duan, Zhaoqing Meng, Hongjing Dong,* and Xiao Wang



Cite This: *ACS Omega* 2022, 7, 46833–46842



Read Online

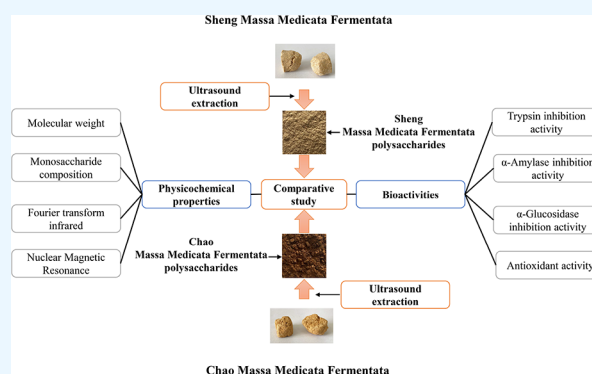
ACCESS |

Metrics & More

Article Recommendations

Supporting Information

ABSTRACT: Two polysaccharides were separately extracted and purified from different types of medicinal slices of Massa Medicata Fermentata (Sheng Massa Medicata Fermentata and Chao Massa Medicata Fermentata). The physicochemical properties of these polysaccharides were studied, including the molecular weight, monosaccharide composition, and glycosidic linkage. Moreover, inhibition of trypsin, α -amylase, and α -glucosidase by the polysaccharides and their antioxidant activity were investigated. Compared with polysaccharides from Sheng Massa Medicata Fermentata, polysaccharides from Chao Massa Medicata Fermentata had a lower molecular weight, higher uronic acid content, and a lower proportion of side chains. Polysaccharides from Sheng Massa Medicata Fermentata displayed stronger trypsin, α -amylase, and α -glucosidase inhibition activity, whereas the antioxidant activity of the polysaccharides from Chao Massa Medicata Fermentata was higher. These results indicated that stir-frying changes the physicochemical properties of the polysaccharides significantly, leading to reduced enzyme inhibition activity and an increase in antioxidant activity. This research provides a guide for the selective application of Massa Medicata Fermentata.



1. PRACTICAL APPLICATION

This work studied and compared chemical, structural, and biological properties of two polysaccharides from Sheng Massa Medicata Fermentata and Chao Massa Medicata Fermentata. It is found that Sheng Massa Medicata Fermentata polysaccharides had better enzyme inhibition activity, which indicated that Sheng Massa Medicata Fermentata polysaccharides might be worthy of exploration as a potential natural compound to treat acute pancreatitis, hyperglycemia, and hyperacidity. Chao Massa Medicata Fermentata polysaccharides had better effects in antioxidant activity indicating that it had greater potential application in the treatment of oxidative damage caused by diseases or as a natural anti-aging agent to delay human aging. The research offered a new perspective on the application of Massa Medicata Fermentata polysaccharides.

2. INTRODUCTION

Massa Medicata Fermentata (MMF), also called Liu Shen Qu in Chinese, is a famous traditional Chinese medicine first recorded in the Treatise on Chinese Herbal Nature (Yaoping Lun).¹ MMF consists of *Artemisia caruifolia* Buch.-Ham. ex Roxb., *Polygonum hydropiper* L., *Xanthium strumarium* L., red bean, Armeniacae Amarum Semen, wheat flour, and wheat bran, which is fermented at a specific temperature and moisture level.² MMF can ameliorate the symptoms of

dyspepsia by regulating the homeostasis of the brain–gut–microbiota axis, treating gastrointestinal inflammation, and improving intestinal microflora disturbances.^{1–3} Digestive enzymes and lactic acids in MMF are considered to be bioactive constituents of MMF with only a few studies focusing on the function of polysaccharides in MMF.⁴ In recent decades, natural polysaccharides in Chinese herbs have received considerable attention because of their promising health-promoting functions, such as anti-tumor, anti-inflammatory, antioxidant, anti-diabetic, radiation-protecting, antiviral, hypolipidemic, and immunomodulatory activities.⁵ Therefore, research examining the polysaccharides in MMF should facilitate the development and application of MMF.

Sheng MMF and Chao MMF are different types of medicinal slices of MMF prepared in the clinic. Sheng MMF is prepared by cutting dried fermented MMF into pieces, whereas Chao MMF is prepared by stir-frying Sheng MMF in a hot pot until a burnt flavor is released.⁶ In traditional Chinese

Received: September 13, 2022

Accepted: November 24, 2022

Published: December 7, 2022



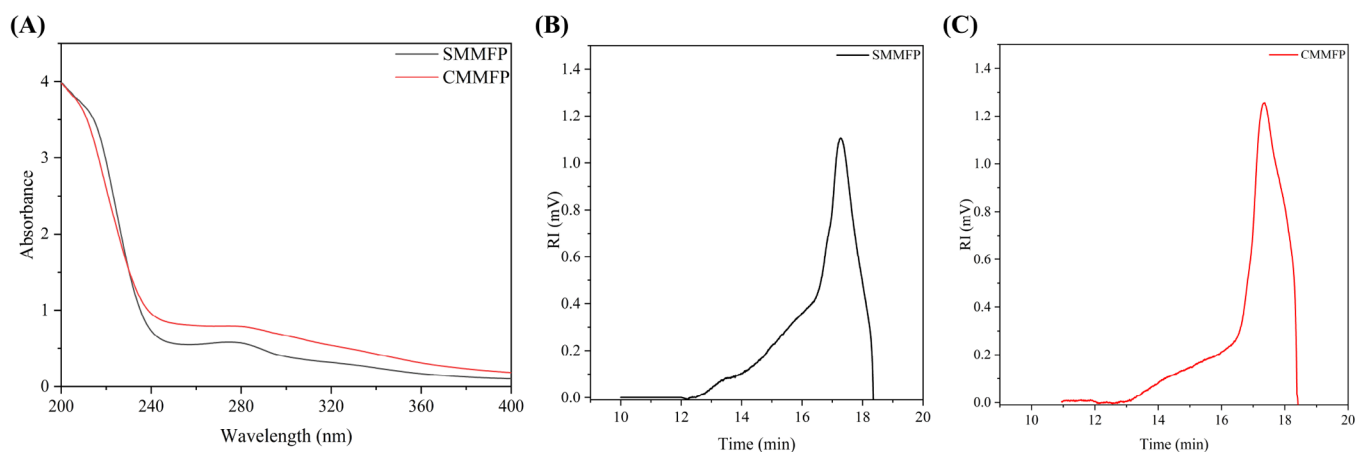


Figure 1. UV spectra of SMMFP and CMMFP (A). High-performance gel permeation chromatograms of SMMFP (B) and CMMFP (C).

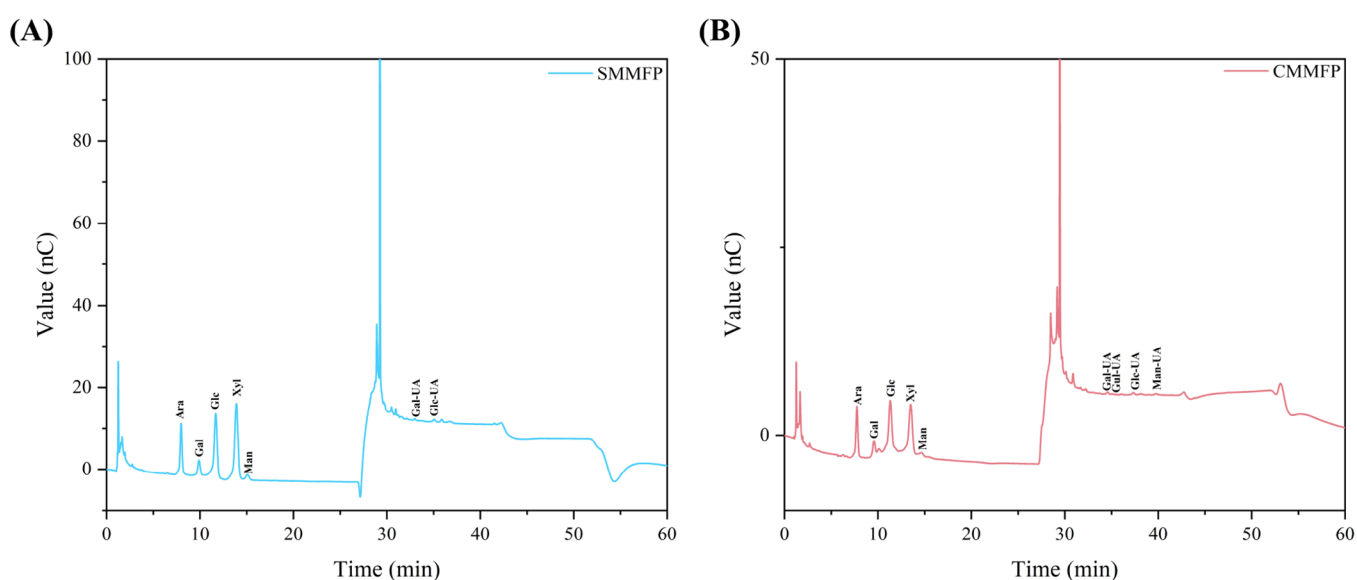


Figure 2. Ion chromatograms of the monosaccharide composition for SMMFP (A) and CMMFP (B).

medicine theory, stir-frying is considered to promote fragrance and invigorate the spleen. Thus, Chao MMF has been found to have higher activity compared with Sheng MMF in invigorating the spleen.⁷ Previous studies suggested that numerous complex chemical reactions occur during stir-frying, such as hydrolysis, oxidation, displacement, isomerization, and decomposition, leading to changes in the medicinal properties of MMF.⁸ These reactions would also occur in polysaccharides, leading to changes in the molecular weight distribution, viscosity, conformation, monosaccharide composition, and bioactivity of the polysaccharides.⁹

The structural properties of polysaccharides are closely related to their bioactivities. To fully clarify the relationship between Sheng MMF polysaccharides (SMMFP) and Chao MMF polysaccharides (CMMFP), the physicochemical properties and bioactivities of SMMFP and CMMFP were studied and compared. The monosaccharide composition, molecular weight (M_w), Fourier-transform infrared (FT-IR) spectra, particle size distribution, microstructure, and nuclear magnetic resonance (NMR) spectra were used to examine their physicochemical properties. In vitro enzymatic inhibition and antioxidant methods were used to assay their bioactivities. This research provides a theoretical basis for the selective

application of MMF and contributes to the investigation and development of polysaccharides from MMF and its processed products.

3. RESULTS AND DISCUSSION

3.1. Ultraviolet (UV) Spectrometry and Molecular Weight Distribution. UV spectra of SMMFP and CMMFP are shown in Figure 1A. No obvious absorption peaks over the 260–280 nm range were observed, suggesting that both polysaccharides contain negligible amounts of proteins after purification with the Sevag reagent.

The M_w of polysaccharides is a crucial index that affects their bioactivities.¹⁰ The M_w values of SMMFP and CMMFP were determined (Figure 1B,C). The M_w of CMMFP (8652 Da) was lower than that of SMMFP (9534 Da). The measured polydispersity index (M_w/M_n) of SMMFP (4.597) was smaller than that of CMMFP (5.607), which may be caused by bond-breaking, a change in the ability to aggregate, and a decrease of β -elimination depolymerization of polysaccharides during the stir-frying process.¹¹

3.2. Monosaccharide Composition. The monosaccharide composition and ratio are important indexes for defining the biological activities of polysaccharides.¹² Figure 2 shows the

ion chromatograms of monosaccharide composition analyses of SMMFP and CMMFP. The analysis of the SMMFP revealed that this polysaccharide was mainly composed of seven kinds of monosaccharides, including arabinose (Ara), galactose (Gal), glucose (Glc), xylose (Xyl), mannose (Man), galacturonic acid (Gal UA), and glucuronic acid (Glc UA). In contrast, the analysis of the CMMFP revealed that this polysaccharide is mainly composed of nine monosaccharides, that is, Ara, Gal, Glc, Xyl, Man, Gal UA, guluronic acid (Glu UA), Glc UA, and mannuronic acid (Man-UA).

The molar ratio of monosaccharides for the SMMFP and CMMFP are listed in Table 1. A comparison of the

Table 1. Molar Ratio of SMMFP and CMMFP

monosaccharide composition	molar ratio (%)	
	SMMFP	CMMFP
Ara	22.24%	23.46%
Gal	7.30%	5.96%
Glc	27.16%	24.85%
Xyl	36.61%	35.46%
Man	4.38%	4.52%
Gal-UA	0.83%	1.65%
Glc-UA	1.48%	1.13%
Gul-UA		0.38%
Man-UA		2.57%

monosaccharide molar ratios for the two polysaccharides revealed that the molar ratios of uronic acids in the CMMFP were higher than those in the SMMFP, indicating that new uronic acids were generated during stir-frying. This difference may be attributed to the oxidation reaction during the stir-frying process with some hydroxyl groups oxidized to carboxyl groups.¹³

3.3. Fourier-Transform Infrared (FT-IR) Spectra. FT-IR spectra of the SMMFP and CMMFP were recorded to obtain more information about the differences between these two polysaccharides (Figure 3). The observed broad band around 3218 cm^{-1} is associated with the stretching vibration of the $-\text{OH}$ group. The observed peak at $\sim 2920\text{ cm}^{-1}$ is related to the C–H asymmetric stretching vibration.¹⁴ The strong signals

at $\sim 1650\text{ cm}^{-1}$ and weak signals at $\sim 1405\text{ cm}^{-1}$ were attributed to asymmetric and symmetric C=O stretching, respectively, of Gal UA, Glc UA, Gul UA, and Man UA.¹³ The band at 1037 cm^{-1} was attributed to the stretching vibration of C–O–C or C–O–H linkages, indicating the presence of glycosidic bonds.¹⁵ The absorption peaks at approximately 937 and 896 cm^{-1} mainly indicated the presence of α -linked and β -linked glycosyl residues and differed between the SMMFP and CMMFP, indicating that the link mode of polysaccharides changed after stir-frying.¹⁶

3.4. Particle Size Distribution. The particle size distributions of the two polysaccharides differed. The diameter of the SMMFP was $(711.43 \pm 1.50)\text{ nm}$, and the particle size distribution was 0.183. The diameter of the CMMFP was $(1035.88 \pm 4.28)\text{ nm}$, and the particle size distribution was 0.296. Good homogeneity was observed for both polysaccharides because the particle size distributions were less than 0.3. However, the diameter of CMMFP was higher than that of SMMFP, suggesting that the thermal motion of the molecules during stir-frying may have caused an increase in the pore wall thickness.¹⁷

3.5. Scanning Electron Microscopy (SEM). The microstructure of the two polysaccharides differed significantly (Figure 4). In general, the surface structure of the holes became more compact after stir-frying. This structural difference arises from the change in the M_w , intermolecular distance, and interconnection during the stir-frying process at high temperatures.⁹ The pore sizes for the SMMFP were larger than those observed for the CMMFP. Moreover, the shape of the pores for the CMMFP was irregular. There were significant differences in the density of the holes between the two samples. In addition, the SMMFP had thinner pore walls than the CMMFP.

3.6. NMR Analysis. The 1D/2D NMR spectra of the SMMFP and CMMFP are shown in Figure S1. In the 1D ^1H spectra of the SMMFP (Figure S1A), peaks at $\delta 4.43$, $\delta 5.16$, $\delta 4.55$, $\delta 4.53$, $\delta 5.07$, $\delta 4.44$, and $\delta 5.21\text{ ppm}$ were assigned to anomeric hydrogens. In the 1D ^{13}C spectra of the SMMFP (Figure S1C), peaks at $\delta 101.69$, $\delta 107.29$, $\delta 97.55$, $\delta 99.65$, $\delta 98.12$, and $\delta 108.21\text{ ppm}$ were assigned to anomeric carbons. In the 2D ^1H – ^{13}C HSQC spectra of the SMMFP (Figure

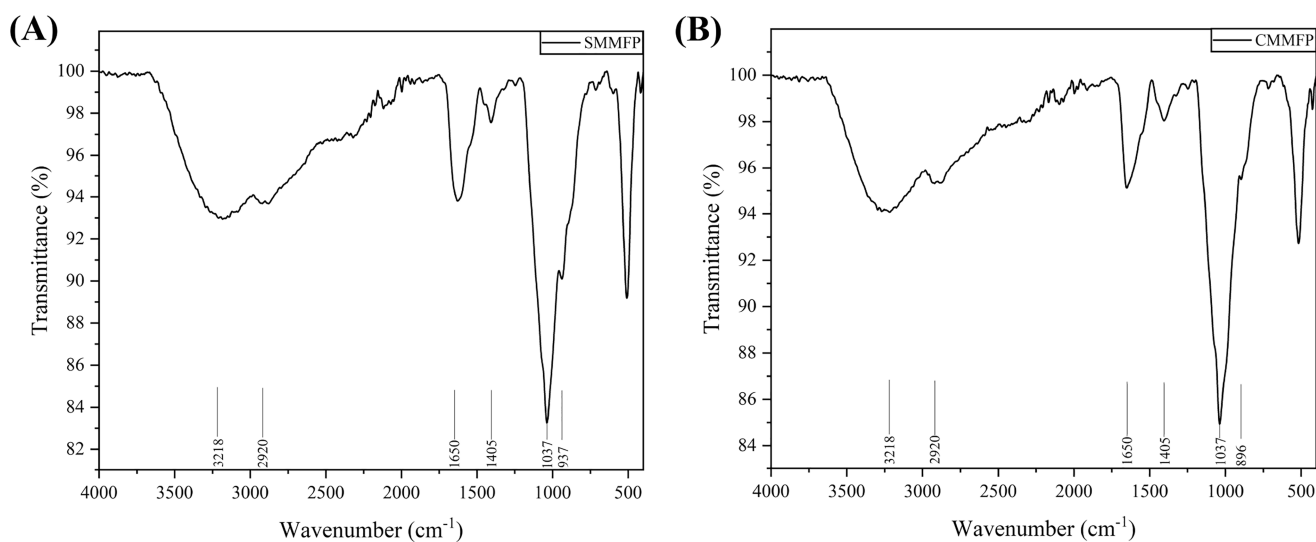


Figure 3. FT-IR spectra of SMMFP and CMMFP.

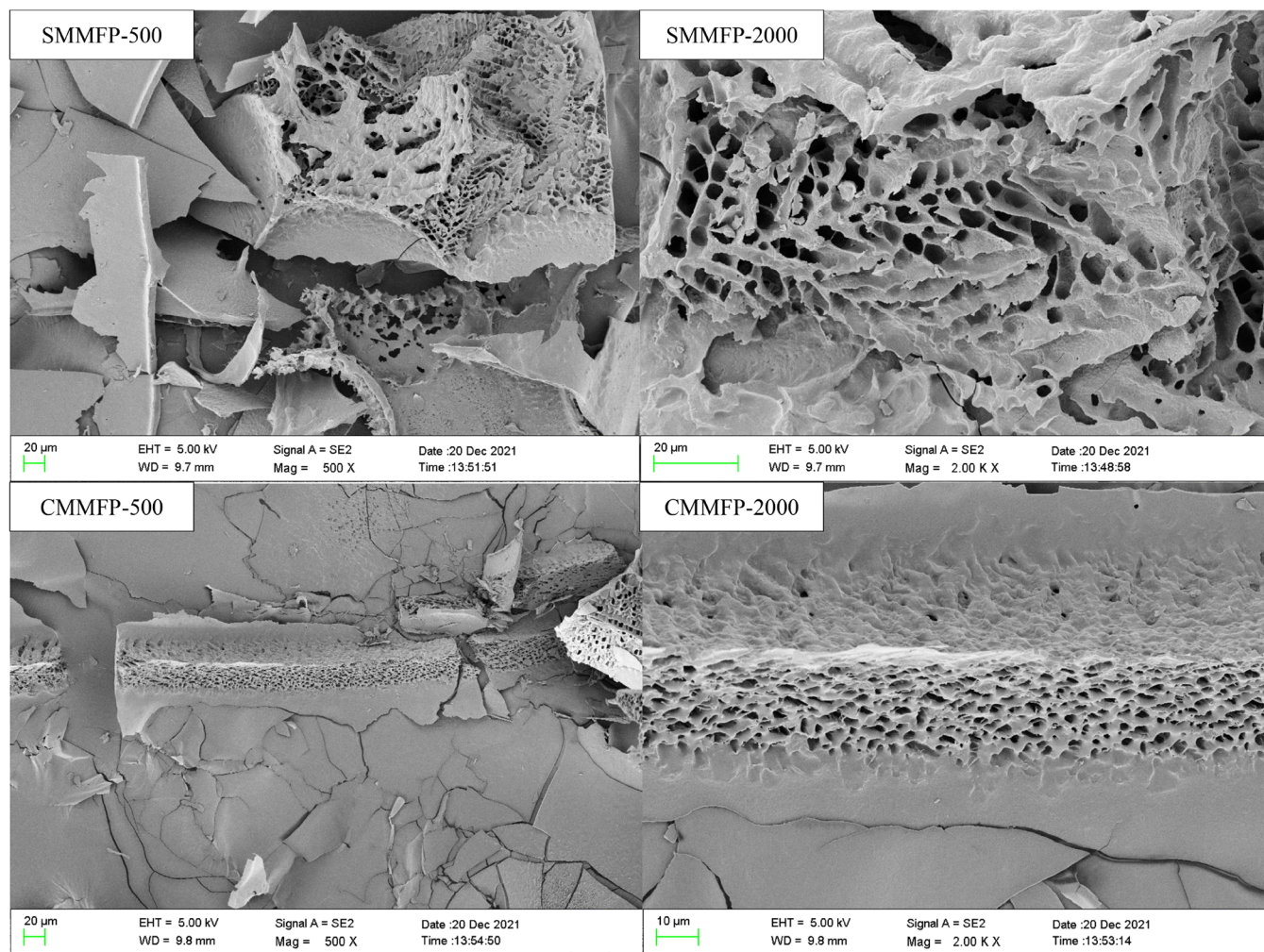


Figure 4. Morphology of the SMMFP and CMMFP observed by SEM.

Table 2. Assignment of Sugar Ring Carbon/Hydrogen Signals of SMMFP and CMMFP

		glycosidic bond		chemical shift δ (ppm)						ref
				1	2	3	4	5	6	
SMMFP	A	1,4-linked-Xylp	H/C	4.43/101.69	3.47/71.14	3.55/78.27	3.54/76.38	3.29/65.03		18
	B	T-linked-Araf	H/C	5.16/107.29	3.89/80.81	3.69/83.87	4.06/81.32	3.78/60.96		19
	C	1,4-linked-Glcp	H/C	4.55/97.55	3.47/71.14	3.78/71.14	3.90/78.42	3.94/70.32	3.72/60.96	20
	D	1,3,4-linked-Xylp	H/C	4.53/99.65	3.29/73.18	3.50/78.27	3.73/76.13	4.07/62.48		18
	E	1,2-linked-Manp	H/C	5.07/98.12	4.04/78.42	3.80/71.14	3.59/69.10	3.83/73.18	3.91/61.32	21
	F	1,3,6-linked-Galp	H/C	4.44/101.69	3.39/72.67	4.09/84.27	3.90/69.10	3.94/76.74	3.92/71.95	22
	G	1,5-linked-Araf	H/C	5.21/108.21	4.11/80.81	4.05/76.23	4.27/83.87	3.76/75.88		19
CMMFP	A	1,4-linked-Xylp	H/C	4.40/101.82	3.22/73.69	3.55/73.17	3.72/76.23	3.34/62.48		23
	B	T-linked-Araf	H/C	5.20/108.31	4.09/82.38	3.88/76.74	4.24/84.38	3.68/61.98		23
	C	1,3,4-linked-Xylp	H/C	4.44/101.31	3.45/71.14	3.25/73.18	3.70/72.67	3.31/62.48		23
	D	1,4-linked-Glcp	H/C	5.35/99.65	3.53/72.66	3.73/76.23	3.64/77.66	3.84/71.14	3.70/60.96	24
	E	1,3,6-linked-Galp	H/C	4.60/100.16	3.43/71.14	3.56/78.27	3.91/69.10	3.75/76.23	3.73/69.61	20
	F	1,2-linked-Araf	H/C	5.07/107.29	4.08/84.27	4.14/80.81	4.25/84.37	3.90/60.45		25

S1G), seven cross-peaks were observed at δ 4.43/101.69, δ 5.16/107.29, δ 4.55/97.55, δ 4.53/99.65, δ 5.07/98.12, δ 4.44/101.69, and δ 5.21/108.21 ppm. These cross-peaks were marked as A, B, C, D, E, F, and G, respectively (Table 2).

Signals at δ 4.43/3.47, δ 3.47/3.55, δ 3.55/3.54, and δ 5.43/3.29 ppm were observed in the 2D ^1H - ^1H COSY spectra of the SMMFP (Figure S1E). Peaks at δ 4.43/101.69, δ 3.47/71.14, δ 3.55/78.27, δ 3.54/76.38, and δ 3.29/65.10 ppm were

observed in the 2D ^1H - ^{13}C HSQC spectra (Figure S1G) of the SMMFP and were tentatively assigned to H1/C1, H2/C2, H3/C3, H4/C4, and H5/C5 of 1,4-linked-Xylp. Signals at δ 5.16/3.89, δ 3.89/3.69, δ 3.69/4.06, and δ 4.06/3.78 ppm were observed in the 2D ^1H - ^1H COSY spectra (Figure S1E). Peaks at δ 5.16/107.29, δ 3.89/80.81, δ 3.69/83.87, δ 4.06/81.32, and δ 3.78/60.96 ppm were observed in the 2D ^1H - ^{13}C HSQC spectra of the SMMFP (Figure S1G), which were

tentatively assigned to H1/C1, H2/C2, H3/C3, H4/C4, and H5/C5 of T-linked-Araf. Peaks at δ 4.53/3.29, δ 3.29/3.50, δ 3.50/3.73, and δ 3.73/4.07 ppm were observed in the 2D ^1H - ^1H COSY spectra (Figure S1E) of the SMMFP. Peaks at δ 4.53/99.65, δ 3.29/73.18, δ 3.50/78.27, δ 3.73/76.13, and δ 4.07/62.48 ppm were observed in the 2D ^1H - ^{13}C HSQC spectra (Figure S1G) of SMMFP and were tentatively assigned to H1/C1, H2/C2, H3/C3, H4/C4, and H5/C5 of 1,3,4-linked-Xylp. Based on the 2D ^1H - ^1H COSY and 2D ^1H - ^{13}C HSQC spectra of the SMMFP, the peaks at δ 4.55/97.55, δ 3.47/71.14, δ 3.78/71.14, δ 3.90/78.42, δ 3.94/70.32, and δ 3.72/60.96 ppm were tentatively deduced to represent H1/C1, H2/C2, H3/C3, H4/C4, H5/C5, and H6/C6 of 1,4-linked-Glcp. The peaks at δ 5.07/98.12, δ 4.04/78.42, δ 3.80/71.14, δ 3.59/69.10, δ 3.83/73.18, and δ 3.91/61.32 ppm were tentatively deduced to represent 1,2-linked-Manp. The peaks at δ 4.44/101.69, δ 3.39/72.67, δ 4.09/84.27, δ 3.90/69.10, δ 3.94/76.74, and δ 3.92/71.95 ppm were tentatively deduced to represent 1,3,6-linked-Galp. The peaks at δ 5.21/108.21, δ 4.11/80.81, δ 4.05/76.23, δ 4.27/83.87, and δ 3.76/75.88 ppm were tentatively assigned to H1/C1, H2/C2, H3/C3, H4/C4, and H5/C5 of 1,5-linked-Araf.

In the 2D ^1H - ^{13}C HMBC spectra of the SMMFP (Figure S1I), the cross-peaks at δ 4.43/75.38 and δ 4.43/76.13 ppm indicated that H-1 of 1,4-linked-Xylp was related to C-4 of 1,4-linked-Xylp and C-4 of 1,3,4-linked-Xylp, respectively. The cross-peaks at δ 5.16/71.95, δ 5.16/76.38, δ 5.16/78.42, δ 5.16/84.27, and δ 5.16/78.27 ppm indicated that most T-linked-Araf terminals connected with unsubstituted residues and mono-substituted residues. The cross-peaks at δ 4.55/75.88 and δ 4.53/75.88 ppm indicated that C-5 of 1,5-linked-Araf was related to H-1 of 1,4-linked-Glcp and H-1 of 1,3,4-linked-Xylp, respectively. The cross-peak at δ 3.50/101.69 ppm indicated that H-1 of 1,3,6-linked-Galp was related to C-3 of 1,3,4-linked-Xylp. The cross-peaks at δ 5.21/78.27 and δ 3.50/108.21 ppm showed that C-1 of 1,5-linked Ara is connected with C-3 of 1,3,4-linked-Xylp (Table 3).

Similarly, peaks at δ 4.40, δ 5.20, δ 4.44, δ 5.35, δ 4.60, and δ 5.07 ppm were observed in the 1D ^1H spectra of the CMMFP

(Figure S1B), and signals at δ 101.82, δ 108.21, δ 101.31, δ 99.65, δ 100.16, and δ 107.29 ppm were observed in the 1D ^{13}C spectra of the CMMFP (Figure S1D). Signals at δ 4.40/3.22, δ 3.22/3.55, δ 3.55/3.72, and δ 3.72/3.34 ppm were observed in the 2D ^1H - ^1H COSY spectra of the CMMFP (Figure S1F), and these signals were marked as A, B, C, D, E, and F, respectively (Table 2). The peaks at δ 4.40/101.82, δ 3.22/73.69, δ 3.55/73.17, δ 3.72/76.23, and δ 3.34/62.48 ppm observed in the 2D ^1H - ^{13}C HSQC spectra of the CMMFP (Figure S1H) were tentatively assigned to H1/C1, H2/C2, H3/C3, H4/C4, and H5/C5 of 1,4-linked-Xylp. Signals at δ 5.20/4.09, δ 4.09/3.88, δ 3.88/4.24, and δ 4.24/3.68 ppm were observed in the 2D ^1H - ^1H COSY spectra. Peaks at δ 5.20/108.31, δ 4.09/82.38, δ 3.88/76.74, δ 4.24/84.38, and δ 3.68/61.98 ppm observed in the 2D ^1H - ^{13}C HSQC spectra of SMMFP were tentatively assigned to H1/C1, H2/C2, H3/C3, H4/C4, and H5/C5 of T-linked-Araf. Peaks at δ 4.44/3.45, δ 3.45/3.25, δ 3.25/3.70, and δ 3.70/3.31 ppm were observed in the 2D ^1H - ^1H COSY spectra. The peaks at δ 4.44/101.31, δ 3.45/71.14, δ 3.25/73.18, δ 3.70/72.67, and δ 3.31/62.48 ppm observed in the 2D ^1H - ^{13}C HSQC spectra of the SMMFP were tentatively assigned to H1/C1, H2/C2, H3/C3, H4/C4, and H5/C5 of 1,3,4-linked-Xylp. As shown in Figure S1F,H, the cross-peaks at δ 5.35/99.65, δ 3.53/72.66, δ 3.73/76.23, δ 3.64/77.66, δ 3.84/71.14, and δ 3.70/60.96 ppm were tentatively assigned to H1/C1, H2/C2, H3/C3, H4/C4, H5/C5, and H6/C6 of 1,4-linked-Glcp. The cross-peak signals at δ 4.60/100.16, δ 3.43/71.14, δ 3.56/78.27, δ 3.91/69.10, δ 3.75/76.23, and δ 3.73/69.61 ppm were tentatively assigned to H1/C1, H2/C2, H3/C3, H4/C4, H5/C5, and H6/C6 of 1,3,6-linked-Galp. The cross-peaks at δ 5.07/107.29, δ 4.08/84.27, δ 4.14/80.81, δ 4.25/84.37, and δ 3.90/60.45 ppm were tentatively assigned to H1/C1, H2/C2, H3/C3, H4/C4, and H5/C5 of 1,2-linked-Araf.

Likewise, in the 2D ^1H - ^{13}C HMBC spectra of CMMFP (Figure S1J), the cross-peak at δ 4.44/76.23 ppm indicated that H-1 of 1,4-linked-Xylp was associated with C-4 of 1,4-linked-Xylp. The cross-peak at δ 5.20/84.27 ppm suggested that T-linked-Araf was related to C-2 of 1,2-linked-Araf. The cross-peak at δ 4.44/72.67 ppm indicated that H-1 of 1,3,4-linked-Xylp was related to C-4 of 1,3,4-linked-Xylp. The cross-peak at δ 5.35/73.18 ppm suggested that H-1 of 1,4-linked-Glcp was associated with C-3 of 1,3,4-linked-Xylp. The cross-peak at δ 3.25/100.16 ppm was the signal of C-3 of 1,3,4-linked-Xylp connected with C-1 of 1,3,6-linked-Galp (Table 3).

Based on the 1D/2D NMR analysis, type of glycosidic bond, and monosaccharide composition analysis, it could be initially speculated that the SMMFP and CMMFP mainly are arabinoxylan with the main chain of the polysaccharides composed of 1,3,4-linked-Xylp and 1,4-linked-Xylp residues. However, the structure of SMMFP and CMMFP differed with the number of side chains (1,2-linked-Manp) present in the SMMFP being higher than that in the CMMFP, indicating that stir-frying may disrupt the bonds for side chains.

3.7. In Vitro Bioactivity Assays. 3.7.1. Trypsin Inhibition Activity. Trypsin is an important pancreatic protease. Over-expression of trypsin can activate various proteases to initiate auto-digestion, which leads to acute pancreatitis. Trypsin inhibitors are promising agents to treat acute pancreatitis.²⁶ Moreover, recent research has also reported the potential beneficial effects of trypsin inhibitors on obesity and cancer.²⁷

Figure SA,B shows a plot of the trypsin inhibition rate of the SMMFP and CMMFP. A significant difference in inhibition

Table 3. Significant Connections Observed in the HMBC Spectra for Anomeric Proton/Carbon of the Sugar Residues of the SMMFP and CMMFP (δ in ppm)

	sugar residue	H1/C1	observed connectivity	
		$\delta_{\text{H}}/\delta_{\text{C}}$	$\delta_{\text{H}}/\delta_{\text{C}}$	residue
SMMFP	A: 1,4-linked-Xylp	4.43	76.38	A-C4
			76.13	D-C4
	B: T-linked-Araf	5.16	71.95	D-C6/F-C6
			76.38	A-C4
			78.42	C-C4/E-C2
			84.27	F-C3
	C: 1,4-linked-Glcp	4.55	75.88	D-C3
			78.27	D-C3
			75.88	G-C5
			75.88	G-C5
78.27			D-C3	
D: 1,3,4-linked-Xylp	5.21	78.27	D-C3	
		108.21	3.5	D-H3
		3.5	108.21	D-H3
CMMFP	A: 1,4-linked-Xylp	4.4	76.23	A-C4
	B: T-linked-Araf	5.2	84.27	F-C2
	C: 1,3,4-linked-Xylp	4.44	72.67	C-C4
	D: 1,4-linked-Glcp	5.35	73.18	C-C3
	E: 1,3,6-linked-Galp	100.16	3.25	C-H3

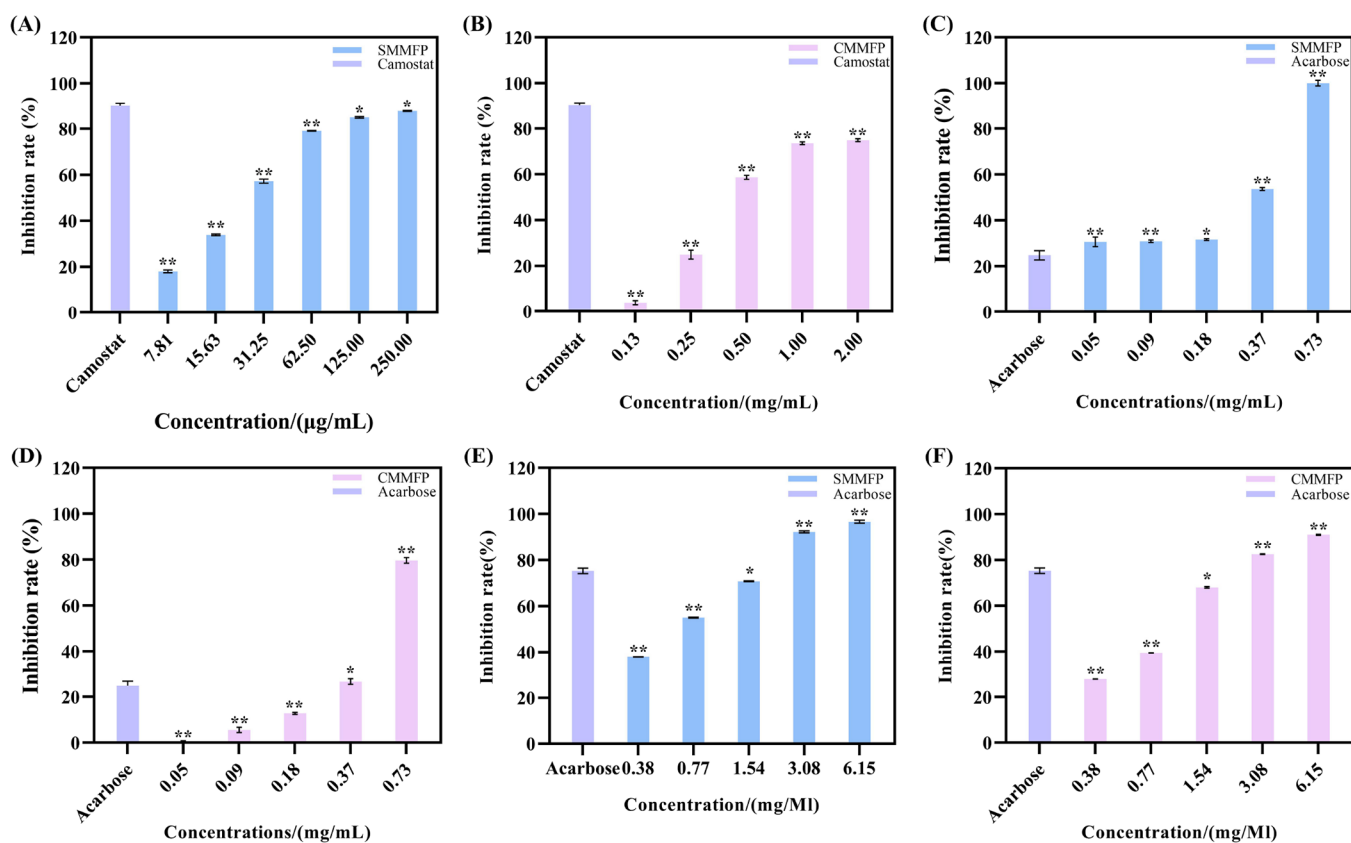


Figure 5. Trypsin (A, B), α -amylase (C, D) and α -glucosidase (E, F) inhibition activity of SMMFP and CMMFP (*: $P < 0.05$, **: $P < 0.01$).

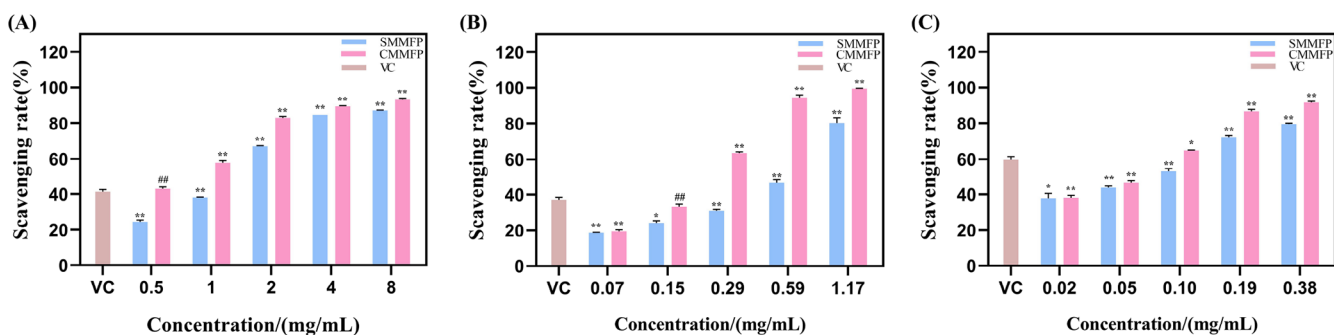


Figure 6. DPPH (A), ABTS (B), and hydroxyl radical (C) scavenging activity of the SMMFP and CMMFP (##: $P > 0.05$, *: $P < 0.05$, **: $P < 0.01$).

was observed between the SMMFP and CMMFP at all concentrations tested. With increasing concentrations of the SMMFP and CMMFP, the maximum trypsin inhibition rate reached $82.33 \pm 0.60\%$ and $81.16 \pm 0.84\%$, respectively. The IC_{50} value of the SMMFP (0.1530 ± 0.0020 mg/mL) was lower than the corresponding value for the CMMFP (0.3332 ± 0.0166 mg/mL), indicating that the SMMFP is a better trypsin inhibitor. This observation may be caused by the broken chemical bonds, the reduced M_w , the change in the monosaccharide ratio and types, and/or the oxidization of hydroxyl groups that occurs while stir-frying at high temperatures.

3.7.2. α -Amylase and α -Glucosidase Inhibition Activity. α -Amylase and α -glucosidase in humans play an essential role in the digestion of starch and absorption of carbohydrates, and inhibitors of these proteins are potentially effective drugs in controlling blood glucose levels in type 2 diabetes mellitus

patients.²⁸ As shown in Figure 5C,D, the α -amylase inhibition rate increased with the increasing polysaccharide concentration with inhibition by SMMFP ($IC_{50} = 0.2124 \pm 0.0033$ mg/mL) being significantly better than that of CMMFP ($IC_{50} = 0.4799 \pm 0.0105$ mg/mL).

As shown in Figure 5E,F, both SMMFP and CMMFP inhibited α -glucosidase activity. The inhibition rate of SMMFP reached 96.63% at 6.15 mg/mL, which was higher than that of CMMFP. In addition, the IC_{50} value of SMMFP (0.6232 ± 0.0011 mg/mL) was lower than that of CMMFP (0.9252 ± 0.0021 mg/mL), indicating that the inhibition activity of SMMFP was better than that of CMMFP.

3.7.3. Antioxidant Activity. The DPPH, ABTS, and hydroxyl radical scavenging activities of SMMFP and CMMFP were examined. The scavenging rate was observed to increase as the concentration of the polysaccharides increased (Figure 6). Interestingly, CMMFP displayed better

DPPH, ABTS, and hydroxyl radical scavenging activities when compared with those of SMMFP. This observation may arise because of the generation of uronic acid in CMMFP samples. For the DPPH scavenging activity (Figure 6A), the IC_{50} values of SMMFP and CMMFP were 1.2720 ± 0.0190 and 0.6687 ± 0.0232 mg/mL, respectively. This difference in IC_{50} values was significant, except for 1.0 mg/mL SMMFP and 0.5 mg/mL CMMFP. For the ABTS scavenging activity (Figure 6B), the IC_{50} values of the CMMFP and SMMFP were 0.1986 ± 0.0042 and 0.5010 ± 0.0149 mg/mL. The IC_{50} values for the ABTS scavenging activity were significantly different between the two polysaccharides, except for 0.15 mg/mL CMMFP. For the hydroxyl radical scavenging activity (Figure 6C), the IC_{50} values of the SMMFP and CMMFP were 0.0607 ± 0.0016 and 0.0461 ± 0.0017 mg/mL, respectively. There was a significant difference at all concentrations of SMMFP and CMMFP. Overall, the antioxidant activity of CMMFP was stronger than that of SMMFP, which indicated that the CMMFP is a good choice for extracting polysaccharides with excellent antioxidant activity from natural sources.

3.8. Relationship between the Structure and Bioactivities of the Polysaccharides. The biological activity of the polysaccharides was markedly associated with their monosaccharide compositions, average M_w , and chemical structures. In this study, the antioxidant activity of CMMFP was stronger than that of SMMFP because SMMFP had a higher average M_w and was limited by steric hindrance.²⁹ SMMFP showed stronger α -amylase and α -glucosidase inhibition than CMMFP because the sugar chains in the polysaccharides of CMMFP degraded during stir-frying. The results are in agreement with a previous study.³⁰ For trypsin inhibition, we hypothesize that the stronger inhibition of trypsin by SMMFP may arise from the rougher morphological properties of SMMFP.³¹

4. MATERIALS AND METHODS

4.1. Samples. Sheng MMF and Chao MMF are all purchased from Kangmei Pharmaceutical Company (Bozhou, Anhui, China). Authenticity of samples is identified by associate professor Hongjing Dong, Shandong Analysis and Test Center.

4.2. Extraction and Purification of Polysaccharides. Sheng MMF (1.0 kg) and Chao MMF (1.0 kg) are separately extracted by ultrasonic-assisted method with a temperature of 80 °C, time of 50 min, power of 250 W, and solid–liquid ratio of 80 mL/g. The extract solution is filtered by a gauze and centrifuged at 10,000 r/min for 10 min at room temperature to collect the supernatant. The supernatant is concentrated by a rotary evaporator at 55 °C, and the crude polysaccharides are purified by an ethanol precipitation method with fourfold volume of ethanol. The precipitate is re-dissolved in 100 mL of distilled water and mixed with the same volume of the Sevag reagent (chloroform/*n*-butanol (4:1, *v/v*)). After being fully shaken for 30 min, the mixture is separated by centrifuging for 10 min at 4000 r/min. This process is repeated five times to remove the protein completely in polysaccharides. Then, the water solution is concentrated by a rotary evaporator at 55 °C to remove residual organic solvents and dialyzed in purified water for 24 h to remove low-molecular compounds. Finally, the dialyzed solution is lyophilized, yielding Sheng MMF polysaccharides (SMMFP) and Chao MMF polysaccharides (CMMFP), separately.

4.3. Measurement of Ultraviolet (UV) Spectra. SMMFP and CMMFP are dissolved in purified water to obtain their aqueous solutions with a concentration of 2 mg/mL. The UV spectra of the solution are measured at a wavelength between 200 and 400 nm using a UV-2450 ultraviolet–visible full-wavelength scanning spectrophotometer (Shimadzu, Japan).

4.4. Molecular Weight Distribution of Polysaccharides. The average molecular weight (M_w) of crude polysaccharides is determined using an Agilent PL-GPC 50 (Agilent Technologies, Amstelveen, Netherlands) apparatus equipped with a refractive index detector (RID, G1362A) and an ultrahydrogel linear column (300 mm \times 7.8 mm i.d., Waters Corporation, MA, USA).³² The sample solution is prepared by dissolving 1.0 mg of polysaccharides in 1.0 mL of purified water. After being treated with a 0.22 μ m membrane filter, 20 μ L of sample solution is injected into a chromatographic system. The mobile phase is 0.02 M KH_2PO_4 (pH 6.0), the flow rate is 0.6 mL/min, the column temperature is 35 °C, and the detector temperature is 45 °C.

Agilent GPC software A.02.01 is applied to process data. The relationship between M_w and the elution volume is built according to a previously reported study.³³ Preliminary calibration is conducted using dextrans with various molecular weights (5, 12, 50, 150, 210, and 410 kDa) as references. The M_w of the sample is estimated by the calibration equation established above.

4.5. Monosaccharide Composition Analysis. Monosaccharide composition analysis is operated according to published research.³⁴ First, the samples (about 5 mg) are hydrolyzed using 2.5 mL of trifluoroacetic acid (2 mol/L) at 121 °C for 2 h in a sealed tube. After drying, the residue is re-dissolved in methanol and dried to remove residue trifluoroacetic acid; this operation is repeated five times. After that, the residue is re-dissolved in deionized water and filtered with a 0.22 μ m membrane filter for further measurement.

The sample solutions are analyzed by high-performance anion-exchange chromatography (HPAEC) on a CarboPac PA-20 anion-exchange column (3.0 \times 150 mm, 10 μ m; Dionex, USA) using a pulsed amperometric detector (PAD; Dionex ICS 5000 system, USA). The flow rate is 0.5 mL/min. The injection volume is 5 μ L. The solvent system is composed of solvent A (0.1 mol/L NaOH) and solvent B (0.1 mol/L NaOH, 0.2 mol/L NaAc). The column is eluted using the gradient mode as follows: 0 min, 95%A; 30 min, 80%A; 30.01 min, 60%A; 45 min, 60%A. The data is processed using Chromeleon 7.2 Chromatography Data System software (CDS, Thermo Scientific, USA). The content of each monosaccharide is calculated by the one-point external standard method according to the peak area and content of reference.

4.6. Measurement of Fourier Transform Infrared (FT-IR) Spectra. Approximately 1.0 mg of polysaccharides is mixed with 150.0 mg of KBr powder then ground and pressed into 1 mm pellets for analysis. The IR spectra is recorded in the range of 400–4000 cm^{-1} using Fourier transform infrared spectroscopy (SENSOR 27, Bruker, Germany).

4.7. Scanning Electronic Microscope (SEM). The dried polysaccharide samples are mounted on a metal stub and sputtered. The polysaccharides samples are coated with a 100 nm gold film, and the morphological property is observed on a SUPRA 55 thermal field-emission scanning electron microscope (Carl Zeiss AG, Germany).

4.8. Particle Size Distribution. The particle diameters of crude polysaccharides are measured using a NanoBrook particle sizer and zeta potential analyzer (NanoBrook Omni, Brookhaven Instruments Corporation, USA). Briefly, 5.0 mg of the polysaccharide sample is dissolved in 10 mL of deionized water and stirred overnight. The solution is put into an ultrasonic cleaner at 350 W for 10 min and placed in a cuvette and scanned with a laser particle-size analyzer.

4.9. NMR Analysis. The dried SMMFP (60.0 mg) and CMMFP (60.0 mg) are dissolved in 0.5 mL of D₂O for NMR analysis. The NMR including 1D ¹H, 1D ¹³C, 2D COSY, 2D HSQC, and 2D HMBs are spectra recorded at 600 MHz for ¹H on a Varian INOVA 600 spectrometer (Varian, Palo Alto, USA) at 300 K using tetramethyl silane (TMS) as an internal standard.

4.10. In Vitro Bioactivity Assays. **4.10.1. Trypsin Inhibition Activity.** Trypsin inhibition activity is determined using *N*- α -benzoyl-DL-arginine-*p*-nitroanilide (BAPNA) as a substrate according to a published method with small modifications.³⁵ In brief, 50.0 μ L of trypsin (1 mg/mL) is first pre-incubated with an equal volume of the polysaccharide solution for 60 min at 25.0 °C. Subsequently, 2.0 mL of BAPNA aqueous solution (1 mmol/L) and 1.5 mL of Tris-HCl buffer (0.1 mol/L, pH 8.0, 50 mmol/L CaCl₂) are added and incubated for 120 min at 25.0 °C. The trypsin inhibition activity is measured by the increase of UV absorbance at 405 nm. In the control group, the polysaccharide solution is replaced by an equal volume of PBS solution. In the background group, all reagents are replaced by an equal volume of PBS solution except for polysaccharides. The trypsin inhibitory activity is calculated using the following formula:

$$\text{trypsin inhibition rate} = \left(1 - \frac{A_{\text{test}} - A_{\text{background}}}{A_{\text{control}}} \times 100\% \right)$$

GraphPad Prism 8 software is used to calculate IC₅₀ values. Camostat mesylate (0.625 μ g/mL) (Shanghai Yuanye Bio-Technology Co., Ltd.) is used as a positive control.

4.10.2. α -Amylase Inhibition Activity. The α -amylase inhibition activity is measured according to published research with small modifications.³⁶ Equal volumes (0.5 mL) of polysaccharide solutions (40.0, 20.0, 10.0, 5.0, and 2.5 mg/mL), α -amylase solution (14 U/mL) (Shanghai Yuanye Bio-technology Co., Ltd.), and 2% starch solution (Shanghai Yuanye Bio-technology Co., Ltd.) are mixed fully and co-incubated at 37 °C for 10 min. Afterward, 1 mL of DNS solution (Shanghai Yuanye Bio-technology Co., Ltd.) is added to terminate the reaction. The aqueous solution was heated in boiling water for 10 min and cooled in cold water for 5 min, and 25.0 mL of deionized water is added subsequently. In the control group, the polysaccharide solution is replaced by an equal volume of PBS solution (pH 7.2). In the background group, after the reaction was terminated with DNS, the α -amylase solution is added. In the blank group, the polysaccharide solutions in the background group are replaced by equal volumes of PBS solution. Acarbose (Shanghai Yuanye Bio-technology Co., Ltd.) (1.82 μ g/mL) was used as a positive control.

The absorbance is measured at a wavelength of 540 nm, and the inhibition rate is calculated using the following equation:

α – amylase inhibition rate

$$= \left(1 - \frac{A_{\text{test}} - A_{\text{background}}}{A_{\text{control}} - A_{\text{blank}}} \right) \times 100\%$$

4.10.3. α -Glucosidase Inhibition Activity. An equal volume of the polysaccharide solutions is mixed with 1 mL of α -glucosidase solution (0.5 U/mL) (Shanghai Yuanye Bio-technology Co., Ltd.) and co-incubated for 10 min at 37 °C. Subsequently, 1 mL of 4-nitrophenyl- β -D-glucopyranoside solution (pNPG) (Shanghai Yuanye Bio-technology Co., Ltd.) (5 mmol/L) is added and co-incubated for 20 min at 37 °C. Then, anhydrous ethanol (1 mL) is added to terminate the reaction. After centrifuging at 8000 r/min for 5 min, the absorbance of the supernatant is measured using a UV spectrophotometer at a wavelength of 405 nm. In the control group, polysaccharides are replaced by an equal volume of PBS solution. In the background group, the α -glucosidase solution and pNPG solution are replaced by an equal volume of PBS. Acarbose (0.77 μ g/mL) is used as a positive control.

The inhibition rate is calculated using the following equation:³⁷

α – glucosidase inhibition rate

$$= \left(1 - \frac{A_{\text{test}} - A_{\text{background}}}{A_{\text{control}}} \right) \times 100\%$$

4.10.4. Antioxidant Activity. DPPH scavenging activity by polysaccharides is measured according to published research.³⁸ The Polysaccharide solution (1.0 mL) is mixed with 3.0 mL of DPPH solution (0.1 mmol/L) (Sigma-Aldrich) and incubated in the dark for 20 min. Subsequently, the absorbance at 517 nm is measured using a UV spectrophotometer. In the control group, the polysaccharide solution is replaced by an equal volume of deionized water. In the blank group, DPPH solution is replaced by an equal volume of anhydrous ethanol. Vitamin C (7.5 μ g/mL) (Shanghai Hushi Laboratorial Equipment Co., Ltd.) is used as a positive control, and the scavenging rate is calculated using the following formula:

$$\text{DPPH scavenging rate} = \left(1 - \frac{A_{\text{test}} - A_{\text{blank}}}{A_{\text{control}}} \right) \times 100\%$$

ABTS scavenging activity by polysaccharides is performed according to published research with small modification.³⁹ The polysaccharide solution (0.3 mL) and 3.8 mL of ABTS solution are fully mixed and incubated in the dark for 6 min. In the control group, the polysaccharide solution is replaced by an equal volume of deionized water. In the blank group, the ABTS solution is replaced by an equal volume of deionized water. Vitamin C (Shanghai Hushi Laboratorial Equipment Co., Ltd.) with a concentration of 2.2 μ g/mL is used as a positive control. The UV absorbance at 734 nm is measured, and the scavenging rate is calculated using the following formula:

$$\text{ABTS scavenging rate} = \left(1 - \frac{A_{\text{test}} - A_{\text{blank}}}{A_{\text{control}}} \right) \times 100\%$$

Hydroxyl radical scavenging activity by polysaccharides is performed according to published research.⁴⁰ In the test group, 1 mL of the polysaccharide solution, 0.6 mL of Fe₂SO₄ solution (2 mmol/L), 0.5 mL of H₂O₂ solution (30%), 0.5 mL of salicylic acid (6 mmol/L) (Xiya Chemical Technology

(Shandong) Co. Ltd.), and 0.4 mL of deionized water are mixed and incubated in the dark for 30 min at 37 °C. In the control group, the polysaccharide solution is replaced by an equal volume of deionized water. In the blank group, the H₂O₂ solution (30%) is replaced by an equal volume of anhydrous ethanol. Vitamin C (10 µg/mL) is used as a positive control. The UV absorbance at 510 nm is measured, and the scavenging rate is calculated as follows:

$$\text{hydroxyl radical scavenging rate} = \left(1 - \frac{A_{\text{test}} - A_{\text{blank}}}{A_{\text{control}}} \right) \times 100\%$$

4.11. Statistical Analysis. All measurements were performed in triplicate, and differences among the groups are determined by one-way analysis of variance (ANOVA) using GraphPad Prism 8 software (GraphPad Software, USA). Results are expressed as the means ± standard deviation; $p < 0.05$ indicates a significant difference, and $p < 0.01$ indicates an extremely significant difference.

5. CONCLUSIONS

In summary, the average M_w of MMF polysaccharides decreased and the uronic acid content increased following stir-frying of Sheng MMF. The in vitro antioxidant activity assay results revealed that CMMFP displayed better DPPH, ABTS, and hydroxyl radical scavenging activities than SMMFP. However, SMMFP showed better enzyme inhibition activity. These results indicated that the SMMFP is a potential natural compound suitable for treating acute pancreatitis, hyperglycemia, and hyperacidity, whereas the CMMFP has potential applications in treating oxidative damage caused by diseases or as a natural anti-aging agent to delay human aging.

■ ASSOCIATED CONTENT

SI Supporting Information

The Supporting Information is available free of charge at <https://pubs.acs.org/doi/10.1021/acsomega.2c05932>.

Results of NMR analysis (PDF)

■ AUTHOR INFORMATION

Corresponding Author

Hongjing Dong – Shandong analysis and test center, Qilu university of technology (Shandong academy of science), Jinan, Shandong 250014, P.R. China; College of pharmacy, Qilu University of technology (Shandong academy of science), Jinan, Shandong 250300, P.R. China; orcid.org/0000-0002-7468-9563; Email: donghongjing_2006@163.com

Authors

Shuang Liu – Shandong analysis and test center, Qilu university of technology (Shandong academy of science), Jinan, Shandong 250014, P.R. China; College of pharmacy, Qilu University of technology (Shandong academy of science), Jinan, Shandong 250300, P.R. China

Long Chen – Shandong analysis and test center, Qilu university of technology (Shandong academy of science), Jinan, Shandong 250014, P.R. China; College of pharmacy, Qilu University of technology (Shandong academy of science), Jinan, Shandong 250300, P.R. China

Wenjuan Duan – Shandong analysis and test center, Qilu university of technology (Shandong academy of science),

Jinan, Shandong 250014, P.R. China; College of pharmacy, Qilu University of technology (Shandong academy of science), Jinan, Shandong 250300, P.R. China

Zhaoqing Meng – Shandong Hongjitang Pharmaceutical Group Co., LTD., Jinan, Shandong 250100, P.R. China

Xiao Wang – Shandong analysis and test center, Qilu university of technology (Shandong academy of science), Jinan, Shandong 250014, P.R. China; College of pharmacy, Qilu University of technology (Shandong academy of science), Jinan, Shandong 250300, P.R. China; orcid.org/0000-0003-4236-2483

Complete contact information is available at:

<https://pubs.acs.org/10.1021/acsomega.2c05932>

Author Contributions

S.L.: Conceptualization, methodology, formal analysis, and writing - original draft. L.C.: Validation and writing - review and editing. W.D.: Software. Z.M.: Resources. X.W.: Project administration and funding acquisition. H.D.: Supervision, writing - review and editing, and funding acquisition.

Notes

The authors declare no competing financial interest.

■ ACKNOWLEDGMENTS

This work was supported by the Shandong Major Technological Innovation Project (no. 2021CXGC010508), China Agriculture Research System of MOF and MARA (CARS-21), the innovative team of Jinan (no. 2020GXRC007), and the Science, Education, and Industry Integration Innovation Pilot Project from Qilu University of Technology (Shandong Academy of Sciences) (no. 2022JBZ02-04).

■ REFERENCES

- (1) Xu, M. S.; Fu, Q.; Baxter, A. The components and amylase activity of Massa Medicata Fermentata during the process of fermentation. *Trends Food Sci. Technol.* **2019**, *91*, 653–661.
- (2) Zhang, H.; Gao, S.; Zhang, X.; Meng, N.; Chai, X.; Wang, Y. Fermentation characteristics and the dynamic trend of chemical components during fermentation of Massa Medicata Fermentata. *Arab. J. Chem.* **2022**, *15*, No. 103472.
- (3) Fu, X.; Wang, Q. H.; Kuang, H. X.; Jiang, P. H. Mechanism of Chinese Medicinal-Medicated Leaven for Preventing and Treating Gastrointestinal Tract Diseases. *Digestion* **2020**, *101*, 659–666.
- (4) Wang, H. Y.; Gao, W. Y.; Zhang, L. X. Influence of different processing techniques of Massa Medicata Fermentata on their amylase activity. *China J. Chin. Mater. Med.* **2012**, *37*, 2084–2087.
- (5) Zheng, Q. W.; Jia, R. B.; Ou, Z. R.; Li, Z. R.; Zhao, M. M.; Luo, D. H.; Lin, L. Z. Comparative study on the structural characterization and α -glucosidase inhibitory activity of polysaccharide fractions extracted from *Sargassum fusiforme* at different pH conditions. *Int. J. Biol. Macromol.* **2022**, *194*, 602–610.
- (6) Gao, P. F.; Zhang, W. Y.; Zhou, R. R.; Zhang, Y. C.; Ma, W. W.; Shi, X. Y. Effects of Different Liushen Qu on Digestive Function in Mice. *Chin. Arch. Tradit. Chin. Med.* **2016**, *34*, 362–364.
- (7) Wang, Y. X.; Xu, Y.; Xia, M. Q.; Zhou, Z. L.; Wan, J. Historical Evolution and Variance Analysis of Chinese Drugs Fired to Brown. *Chin. Arch. Tradit. Chin. Med.* **2018**, *36*, 357–360.
- (8) Cai, T.; Qin, K. M.; Cai, B. C. Chemical Mechanism During Chinese Medicine Processing. *Prog. Chem.* **2012**, *24*, 637–649.
- (9) Wang, Y.; Li, X.; Chen, X. T.; Zhao, P.; Qu, Z.; Ma, D.; Zhao, C. C.; Gao, W. Y. Effect of stir-frying time during *Angelica Sinensis* Radix processing with wine on physicochemical, structure properties and bioactivities of polysaccharides. *Process Biochem.* **2019**, *81*, 188–196.

- (10) Sheng, J. W.; Sun, Y. L. Antioxidant properties of different molecular weight polysaccharides from *Athyrium multidentatum* (Doll.) Ching. *Carbohydr. Polym.* **2014**, *108*, 41–45.
- (11) Njoroge, D. M.; Kinyanjui, P. K.; Chigwedere, C. M.; Christiaens, S.; Makokha, A. O.; Sila, D. N.; Hendrickx, M. E. Mechanistic insight into common bean pectic polysaccharide changes during storage, soaking and thermal treatment in relation to the hard-to-cook defect. *Food Res. Int.* **2016**, *81*, 39–49.
- (12) Yan, J. M.; Zhu, L.; Qu, Y. H.; Qu, X.; Mu, M. X.; Zhang, M. S.; Muneer, G.; Zhou, Y. F.; Sun, L. Analyses of active antioxidant polysaccharides from four edible mushrooms. *Int. J. Biol. Macromol.* **2019**, *123*, 945–956.
- (13) Liu, Y.; Luo, M. L.; Liu, F.; Feng, X.; Ibrahim, S. A.; Cheng, L.; Huang, W. Effects of freeze drying and hot-air drying on the physicochemical properties and bioactivities of polysaccharides from *Lentinula edodes*. *Int. J. Biol. Macromol.* **2020**, *145*, 476–483.
- (14) Zhu, S. S.; Qiu, Z. C.; Qiao, X. G.; Waterhouse, G. I. N.; Zhu, W. Q.; Zhao, W. T.; He, Q. X.; Zheng, Z. J. Creating burdock polysaccharide-oleanolic acid-ursolic acid nanoparticles to deliver enhanced anti-inflammatory effects: fabrication, structural characterization and property evaluation. *Food Sci. Hum. Wellness* **2023**, *12*, 454–466.
- (15) Hao, L. M.; Sheng, Z. C.; Lu, J. K.; Tao, R. Y.; Jia, S. R. Characterization and antioxidant activities of extracellular and intracellular polysaccharides from *Fomitopsis pinicola*. *Carbohydr. Polym.* **2016**, *141*, 54–59.
- (16) Li, W. F.; Song, K. D.; Wang, S.; Zhang, C. H.; Zhuang, M. L.; Wang, Y. W.; Liu, T. Q. Anti-tumor potential of astragalus polysaccharides on breast cancer cell line mediated by macrophage activation. *Mater. Sci. Eng. C* **2019**, *98*, 685–695.
- (17) Li, Q.; Li, X. J.; Ren, Z. Y.; Wang, R. J.; Zhang, Y.; Li, J.; Ma, F. Y.; Liu, X. H. Physicochemical properties and antioxidant activity of Maillard reaction products derived from *Dioscorea opposita* polysaccharides. *LWT* **2021**, *149*, No. 111833.
- (18) Yin, J.-Y.; Lin, H.-X.; Li, J.; Wang, Y.; Cui, S. W.; Cui, S. W.; Nie, S.; Xie, M. Structural characterization of a highly branched polysaccharide from the seeds of *Plantago asiatica* L. *Carbohydr. Polym.* **2012**, *87*, 2416–2424.
- (19) Ding, H. H.; Qian, K.; Goff, H. D.; Wang, Q.; Cui, S. W. Structural and conformational characterization of arabinoxylans from flaxseed mucilage. *Food Chem.* **2018**, *254*, 266–271.
- (20) Chen, Y.; Jiang, X.; Xie, H.; Li, X.; Shi, L. Structural characterization and antitumor activity of a polysaccharide from *ramulus mori*. *Carbohydr. Polym.* **2018**, *190*, 232–239.
- (21) Zhang, H.; Zhang, N.; Xiong, Z.; Wang, G.; Xia, Y.; Lai, P.; Ai, L. Structural characterization and rheological properties of β -D-glucan from hull-less barley (*Hordeum vulgare* L. var. *nudum* Hook. f.). *Phytochemistry* **2018**, *155*, 155–163.
- (22) Nyman, A. A. T.; Aachmann, F. L.; Rise, F.; Ballance, S.; Samuelsen, A. B. C. Structural characterization of a branched (1→6)- α -mannan and β -glucans isolated from the fruiting bodies of *Cantharellus cibarius*. *Carbohydr. Polym.* **2016**, *146*, 197–207.
- (23) Guo, R.; Xu, Z.; Wu, S.; Li, X.; Li, J.; Hu, H.; Wu, Y.; Ai, L. Molecular properties and structural characterization of an alkaline extractable arabinoxylan from hull-less barley bran. *Carbohydr. Polym.* **2019**, *218*, 250–260.
- (24) Shi, X.-D.; Li, O.-Y.; Yin, J.-Y.; Nie, S.-P. Structure identification of α -glucans from *Dictyophora echinvolvata* by methylation and 1D/2D NMR spectroscopy. *Food Chem.* **2018**, *271*, 338–344.
- (25) Maity, G. N.; Maity, P.; Dasgupta, A.; Acharya, K.; Dalai, S.; Mondal, S. Structural and antioxidant studies of a new arabinoxylan from green stem *Andrographis paniculata* (Kalmegh). *Carbohydr. Polym.* **2019**, *212*, 297–303.
- (26) Mohacek-Grosec, V.; Bozac, R.; Puppels, G. J. Vibrational spectroscopic characterization of wild growing mushrooms and toadstools. *Spectrochim. Acta, Part A* **2001**, *57*, 2815–2829.
- (27) Lima, V. C. O. D.; Piuvezam, G.; Maciel, B. L. L.; Morais, A. H. D. A. Trypsin inhibitors: promising candidate satietogenic proteins as complementary treatment for obesity and metabolic disorders? *J. Enzyme Inhib. Med. Chem.* **2019**, *34*, 405–419.
- (28) Lv, Q. Q.; Cao, J. J.; Liu, R.; Chen, H. Q. Structural characterization, α -amylase and α -glucosidase inhibitory activities of polysaccharides from wheat bran. *Food Chem.* **2021**, *341*, No. 128218.
- (29) Liu, H.; Xu, J.; Xu, X.; Yuan, Z.; Song, H.; Yang, L.; Zhu, D. Structure/function relationships of bean polysaccharides: A review. *Crit. Rev. Food Sci. Nutr.* **2021**, No. 1946480.
- (30) Wang, Y.; Yang, Z.; Wei, X. Sugar compositions, α -glucosidase inhibitory and amylase inhibitory activities of polysaccharides from leaves and flowers of *Camellia sinensis* obtained by different extraction methods. *Int. J. Biol. Macromol.* **2010**, *47*, 534–539.
- (31) Wang, C.; Santhanam, R. K.; Gao, X.; Chen, Z.; Chen, Y.; Wang, C.; Xu, L.; Chen, H. Preparation, characterization of polysaccharides fractions from *Inonotus obliquus* and their effects on α -amylase, α -glucosidase activity and H_2O_2 -induced oxidative damage in hepatic L02 cells. *J. Funct. Foods* **2018**, *48*, 179–189.
- (32) Feng, L.; Yin, J. Y.; Nie, S. P.; Wan, Y. Q.; Xie, M. Y. Fractionation, physicochemical property and immunological activity of polysaccharides from *Cassia obtusifolia*. *Int. J. Biol. Macromol.* **2016**, *91*, 946–953.
- (33) Nie, S. P.; Xie, M. Y.; Wang, Y. X. Preparation of tea glycoprotein and its application as a calibration standard for the quantification and molecular weight determination of tea glycoprotein in different tea samples by high-performance gel-permeation chromatography. *Anal. Bioanal. Chem.* **2005**, *383*, 680–686.
- (34) Salvador, L. D.; Sugauma, T.; Kitahara, K.; Tanoue, H.; Ichiki, M. Monosaccharide composition of sweetpotato fiber and cell wall polysaccharides from sweetpotato, cassava, and potato analyzed by the high-performance anion exchange chromatography with pulsed amperometric detection method. *J. Agric. Food Chem.* **2000**, *48*, 3448–3454.
- (35) Samiksha; Singh, D.; Kesavan, A. K.; Sohal, S. K. Purification of a trypsin inhibitor from *Psoralea corylifolia* seeds and its influence on developmental physiology of *Bactrocera cucurbitae*. *Int. J. Biol. Macromol.* **2019**, *139*, 1141–1150.
- (36) Zhou, X. L.; Yang, Q. M.; Kong, Y. Q.; Liu, Y. H. Inhibitory Effect of Polysaccharides from *Rosa Roxburghii* Tratt on Activity of α -Amylase. *Food Sci. Technol.* **2020**, *45*, 207–212.
- (37) Ghani, U.; Nur-E-Alam, M.; Yousaf, M.; Ul-Haq, Z.; Noman, O. M.; Al-Rehaily, A. J. Natural flavonoid α -glucosidase inhibitors from *Retama raetam*: Enzyme inhibition and molecular docking reveal important interactions with the enzyme active site. *Bioorg. Chem.* **2019**, *87*, 736–742.
- (38) Cao, H. X.; Wu, D.; Wang, X. S.; Bai, Y.; Wu, Q.; Dai, Y. G. Degradation of *Auricularia auricula* Polysaccharide and Antioxidant Activity of Its Products. *Food R&D* **2022**, *43*, 15–21.
- (39) Hu, D.; Wang, Y.; Yang, M.; Li, S. Study on extraction and antioxidant activity of polysaccharides from *Catathelasma ventricosum* in Yunnan Province. *China Condiment* **2022**, *47*, 78–83.
- (40) Liu, P.; Li, D.; Ji, H. Y.; Jia, X. L.; Tian, L. Purification and Antioxidant Activity Characterization of *Fructus lycii* Polysaccharides. *Food R&D* **2022**, *43*, 111–116.